

Available online at www.sciencedirect.com

Procedia Engineering 10 (2011) 409–414

Engineering
Procedia

ICM11

Effect of alloying elements on ductile-to-brittle transition behavior of high-interstitial-alloyed 18Cr-10Mn austenitic steels

B. Hwang^{a,*}, T-H. Lee^a, S-J Kim^a^a*Korea Institute of Materials Science, 797 Changwondaero, Changwon, 641-831, Korea*

Abstract

A study has been made on the effect of alloying elements on ductile-to-brittle transition (DBT) behavior of high-interstitial-alloyed 18Cr-10Mn austenitic steels containing similar amount of N + C. All the steels exhibited a DBT behavior regardless of chemical composition and their DBT temperature (DBTT) was affected by austenite stability and interstitial elements such as N and C. With the exception of a stable austenitic steel, the DBTT measured by Charpy impact tests appeared to be higher than that calculated by an empirical equation depending on N and C. The DBTT of the N alloyed steels was increased with decreasing austenite stability, which is attributed to deformation-induced martensitic transformation occurred at low temperatures, and thus the difference between measured and calculated DBTTs showed a good correlation with austenite stability. At the same content of alloying elements, on the other hand, the N + C alloyed steel had a lower DBTT than the N alloyed steel, presumably because the combined addition of N + C enhances the metallic component of interatomic bonds and also lower N content contributes to the decrease of DBTT.

© 2011 Published by Elsevier Ltd. Open access under [CC BY-NC-ND license](https://creativecommons.org/licenses/by-nc-nd/4.0/).

Selection and peer-review under responsibility of ICM11

Keywords: ductile-to-brittle transition; high-interstitial-alloyed; austenitic steels; alloying elements

1. Introduction

In recent years, high-interstitial-alloyed austenitic steels as a replacement of high-nitrogen austenitic steels have drawn increasing attention because of a positive synergistic effect of N and C on corrosion and mechanical properties such as yield strength, fracture toughness, resistance to creep and fatigue without significant change in ductility [1-4]. The new alloy system utilizing C as a major alloying element together with N have been also proposed in a cost-effective way to overcome high-pressure metallurgy for increasing solubility of N in iron melts. It was found that the combination of N and C effectively stabilizes austenite phase and increases their individual interstitial solubility [3]. In high-interstitial-alloyed austenitic steels with combined addition of N + C, free electron concentration is much greater than the simple sum of the individual contribution. According to Gavriljuk *et al* [4], the substitution of N or C by N + C increases the density of electron states at the Fermi level, which corresponds to an increased concentration of free electrons and to an enhanced metallic character of interatomic bonds. These changes in the electron structure by N + C promote short-range atomic ordering concerned with the increased

* Corresponding author. Tel.: +82-55-280-3437; fax: +82-55-280-3599.

E-mail address: entropy0@kims.re.kr.

thermodynamic stability of solid solutions and thus lead to the increase in strength with good plasticity and toughness, which allows to develop ultra-high strength corrosion-resistant steels with a lean composition of costly elements.

Several important points regarding the ductile-to-brittle transition (DBT) behavior of high-nitrogen austenitic steels have already been established. Nitrogen alloying causes DBT by cleavage-like brittle fracture which generally does not occur in conventional fcc metals [5,6]. The DBT temperature (DBTT) depends mainly on N content due to unique influence of N [7,8]. However, there is not much known about the DBT behavior of high-interstitial-alloyed austenitic steels with combined addition of N + C. Recently, Speidel and Bernauer [9,10] reported that the DBTT of high-interstitial-alloyed austenitic steels is not only affected by N content but also by C content to a smaller extent. The aim of the present study is to elucidate the DBT behavior of high-interstitial-alloyed austenitic steels with different alloying elements.

2. Experimental Procedure

The materials used in this study were four high-interstitial-alloyed 18Cr-10Mn steels with N + C content of about 0.6 wt. %. They were melted using a pressurized vacuum-induction furnace (VIM 4 III-P, ALD, Germany) and hot rolled to 12 mm thick plate. They were subsequently annealed at 1100°C for 30 min and water quenched to obtain a fully austenite structure. After the annealing treatment, microstructural observations revealed that the matrix was austenite single-phase free of precipitation. The grain size measured by a linear intercept method was between 50 and 80 μm based on electron back-scatter diffraction (EBSD) analysis.

For convenience, the A, B, and C steels containing solely N are referred as N alloyed steels, and the D steel having both N and C is referred as N + C alloyed steel. The chemical composition, nitrogen partial pressure, and austenite stability of the high-interstitial-alloyed 18Cr-10Mn austenitic steels with different alloying elements are provided in Table 1. The M_{d30} temperature, at which the austenitic steel has 50% transformed α' -martensite after a deformation of 30% in tensile testing, was used as a quantitative criterion to evaluate austenite stability [11,12]. The lower M_{d30} temperature is, the higher is austenite stability. Among the steels investigated, the A steel has the highest austenite stability because its M_{d30} temperature is very low due to the higher content of substitutional elements such as Ni and Mo.

Table 1. Chemical composition, nitrogen partial pressure, and austenite stability

Alloy system	Steel	Chemical composition (wt. %)						C+N	$P_{N_2}^*$ (bar)	M_{d30}^{**} (°C)	Austenite stability ^{***}
		Cr	Mn	Ni	Mo	C	N				
N alloyed	A	17.94	9.08	3.56	2.71	0.07	0.54	0.61	3.2	-211.0	Stable
	B	18.46	9.49	0.44	0.28	0.04	0.58	0.62	3.0	-87.2	Metastable
	C	18.57	10.01	2.05	-	0.02	0.53	0.55	2.5	-99.5	Metastable
N + C alloyed	D	18.34	10.08	2.10	-	0.23	0.34	0.57	1.1	-110.0	Metastable

* Nitrogen partial pressure in pressurized vacuum induction melting process.

** $M_{d30}=551-462[\%N+\%C]-9.2[\%Si]-8.1[\%Mn]-13.7[\%Cr]-29[\%Ni+\%Cu]-18.5[\%Mo]-68[\%Nb]$

*** High-interstitial-alloyed steels which undergo deformation-induced martensitic transformation during Charpy impact testing at a temperature ranging from -196 to +100 °C are regarded as metastable.

Subsize round tensile specimens with a gage diameter of 6.3 mm and a gage length of 25.4 mm were prepared and tested at room temperature with a crosshead speed of 5 mm/min using a 10-ton universal testing machine (INSTRON 5882, Canton, USA). Charpy impact tests were performed on standard Charpy V-notch specimens with a 10 × 10 × 55 mm size at temperatures ranging from -196 to +100 °C in accordance with ASTM E23-02. To reduce errors in data interpretation, a regression analysis for absorbed energy plotted as a function of test temperature was also done by a hyperbolic tangent curve-fitting method. Based on the data obtained from the regression analysis, upper-shelf energy (USE) and DBTT were determined. After the Charpy impact tests, the fracture surface and cross-sectional area of the tested specimens were examined using optical and scanning electron microscopes (SEM, model: JSM-7001F, JEOL, Tokyo, Japan).

3. Results and Discussion

3.1. Tensile and Charpy impact properties

Figures 1 and 2 present the absorbed energy and overall fracture surfaces of Charpy impact specimens tested at various temperatures. The tensile and Charpy impact test results are summarized in Table 2. The yield and tensile strengths were varied with chemical composition and the total elongation was nearly the same as approximately 70%. The absorbed energy continuously decreased with decreasing test temperature, showing a DBT behavior unlike conventional fcc metals. The overall fracture appearances reveal that the Charpy impact specimens tested at temperatures below DBTT were hardly deformed, whereas some shear lips were occasionally observed in the specimens tested at -150 and -120 °C, particularly in the A and D steels (Fig. 2). The upper-shelf energy was between 280 and 360 J/cm². The A steel showed an excellent mechanical property of the highest USE and the lowest DBTT together with good tensile properties compared with the other steels (Table 2).

On the other hand, the A steel with the highest austenite stability has about the same DBTT as that calculated by an equation depending on N and C ($DBTT = 300[\%N] + 100[\%C] - 303$ (°C)), whereas the B, C, and D steels with lower austenite stability have higher DBTT by approximately 60 °C than the calculated DBTT. It seems that austenite stability practically affects the DBTT. If austenite stability is insufficient due to low content of substitutional elements, deformation-induced martensitic transformation (DIMIT) can readily occur and thus deteriorate low-temperature toughness, which contributes to the increase in DBTT [13].

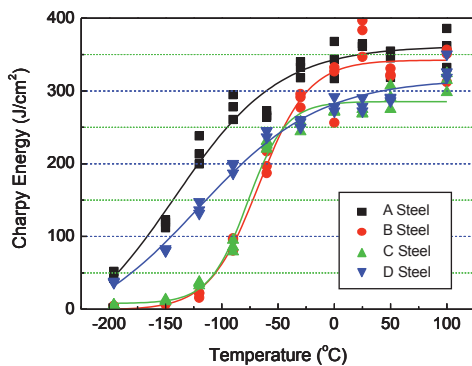


Fig. 1. Charpy impact energy plotted as a function of test temperature.

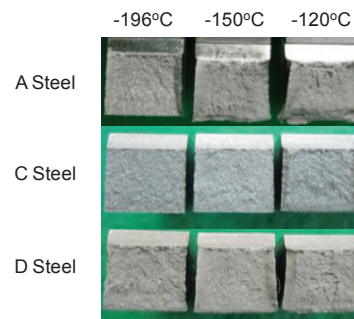


Fig. 2. Overall fracture appearance of the Charpy impact specimens tested at low temperatures.

Table 2. Tensile and Charpy impact properties.

Alloy System	Steel	Tensile properties			Charpy impact properties		
		YS (MPa)	TS (MPa)	El. (%)	USE (J/cm ²)	DBTT (°C)	DBTT (°C)*
N Alloyed	A	532	920	67	362	-141	-133
	B	538	921	70	341	-67	-126
	C	462	839	67	285	-77	-142
N + C Alloyed	D	440	864	70	317	-121	-178

* Calculated by an empirical equation, $DBTT = 300[\%N] + 100[\%C] - 303$ (°C)

3.2. Fractography and deformed microstructure

Figure 3 shows SEM fractographs of Charpy impact specimens tested at various temperatures. When tested at +20 °C, all the steels were fractured in ductile mode with coalescence of microvoids. The A and D steels still exhibit ductile mode at -120 °C, while the C steel had a mixture fracture mode consisting of shallow microvoids

intermingled with some areas of transgranular fracture at $-120\text{ }^{\circ}\text{C}$. However, the fracture surface of the specimens tested at $-196\text{ }^{\circ}\text{C}$ was composed mostly of transgranular brittle fracture areas. It is known that the transgranular flat facets are $\{111\}$ crystallographic planes and the formation of slip steps by crack propagation along parallel planes indicates a plastic deformation prior to the $\{111\}$ fracture [6,14]. Slip traces with angles 60° are visible on the flat facets, unlike conventional ferritic steels fractured at low temperatures. Figure 4 provides optical micrographs of the cross-sectional area beneath the fracture surface of Charpy impact specimens tested at $-120\text{ }^{\circ}\text{C}$ for the C and D steels. Dense planar lines are frequently observed in the vicinity of the fracture surfaces. They are regarded as stacking fault, slip band, deformation twin, or ε -martensite, which is attributed to plastic deformation near the fracture surface [5].

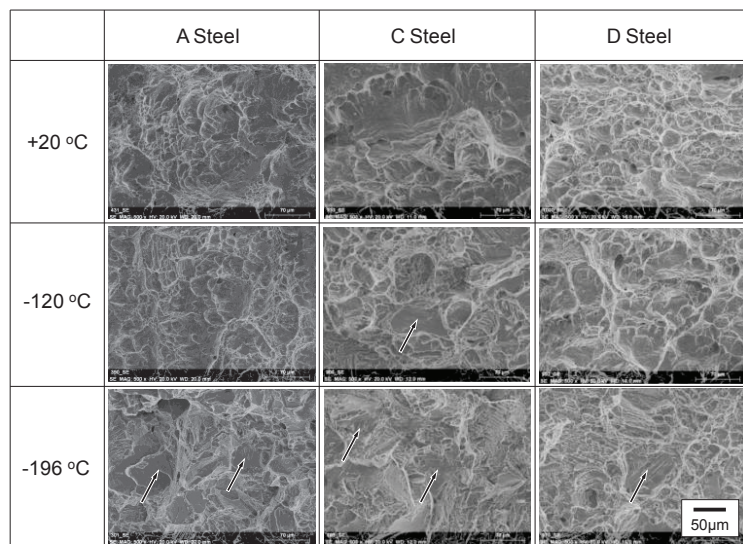


Fig. 3. SEM fractographs of Charpy impact specimens tested at -196°C , -120°C , and $+20^{\circ}\text{C}$. Arrows indicate transgranular brittle facets.

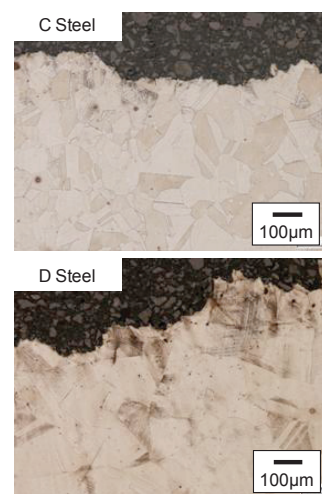


Fig. 4. Optical micrographs of the cross-sectional area beneath the fracture surface of Charpy impact specimens tested at $-120\text{ }^{\circ}\text{C}$.

3.3. Ductile-to-brittle transition temperature (DBTT)

According to our previous study on deformation behavior of high-interstitial-alloyed austenitic steels [15], γ (fcc) \rightarrow ε -martensite (hcp) \rightarrow α' -martensite (bct) transformation sequentially occurs in alloys with N + C content below 0.5 wt. %. Generally, the deformation-induced martensitic transformation is affected by chemical composition, temperature, plastic strain, applied stress state, grain size, and strain rate [12,16]. In this study, ferritescope (model: FMP30, Helmut Fisher GmbH & Co., Sindelfingen, Germany) was used to measure the amount of martensite formed on the fracture surface of Charpy impact specimens tested at various temperatures (Table 3). Very little martensite was found in the A steel with higher austenite stability at any temperature, while it was frequently detectable in the other steels which have lower austenite stability due to low content of substitutional elements such as Mn, Ni, and Mo. This implies that some austenites in the steels with low austenite stability may readily transform to martensite by plastic deformation occurred during Charpy impact tests at low temperatures. The amount of transformed martensite seems to be influenced by the test temperature and associated austenite stability [11-13,16,17].

On the other hand, the DIMT and subsequent transformation toughening have been studied to improve the toughness in a wide variety of materials and may be a promising way to design alloys with high strength and toughness [12-18]. This has been proved theoretically and experimentally over the past decades in both ferrous alloys and ceramic materials. There are some differences in the transformation toughening in these two types of materials. Antolovich [18] has proposed that the net contribution of DIMT to toughness depends on the fracture properties of new phase and the energy dissipated during the transformation process. In steels martensite is more

susceptible to crack propagation than the parent austenite. The energy absorbed during the formation of martensite seems to be negligible because the amount of martensite formed on the fracture surface is too small in the present study. Based on these results, it can be suggested that the contribution of DIMT to the toughness of high-interstitial-alloyed austenitic steels is negative.

Table 3. Amount of martensite on the fracture surface of Charpy impact specimens (Unit: %)

Alloy System	Specimen	Test temperature (°C)									
		-196	-150	-120	-90	-60	-30	0	+20	+50	+100
N Alloyed	A	-	0.26	-	-	-	-	-	-	-	-
	B	0.48	0.47	0.59	0.85	0.93	1.05	0.44	-	-	-
	C	0.42	0.45	0.45	0.45	0.39	0.32	-	-	-	-
N + C Alloyed	D	0.37	0.41	0.50	0.38	-	-	-	-	-	-

Figure 5 compares DBTT measured by Charpy impact test with that calculated by an empirical equation for high-interstitial-alloyed Cr-Mn austenitic steels. In the case of A steel with the highest austenite stability, the measured DBTT is nearly the same as that calculated by an equation ($DBTT = 300[\%N] + 100[\%C] - 303$ (°C)) like data published in literatures [6,7,10,13]. However, the B, C, and D steels with lower austenite stability have a large difference between the measured and calculated DBTTs. This indicates that a reduction in austenite stability deteriorates low-temperature toughness due to the negative contribution of DIMT and thus leads to a significant increase in DBTT. Figure 6 exhibits a relationship between the difference in the measured and calculated DBTTs ($\Delta DBTT$) and the M_{d30} temperature obtained from Nohara's equation [11]. The difference in the DBTTs increases in linear proportion to M_{d30} temperature. Based on these results, it is suggested that austenite stability plays an important role in the DBTT of high-interstitial-alloyed austenitic steels. On the other hand, the DBTT of the D steel (N + C alloyed steel) is lower than that of the C steel (N alloyed steel) at the same interstitial content of 0.6 wt.% N + C, which is probably because the combined addition of N + C enhances the metallic component of interatomic bonds and thus increases plasticity and impact toughness [4].

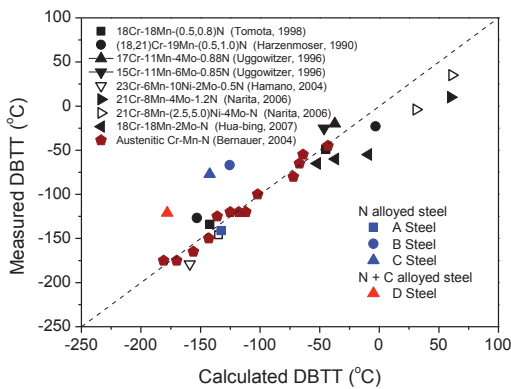


Fig. 5. Comparison of ductile-to-brittle transition temperatures (DBTTs) measured by Charpy impact tests and calculated by an empirical equation.

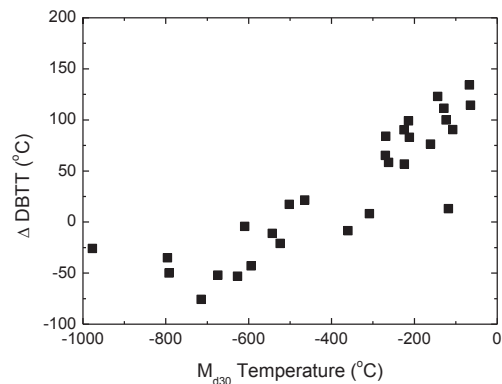


Fig. 6. Relationship between the difference in measured and calculated DBTTs ($\Delta DBTT$) and the M_{d30} temperature obtained from Nohara's equation [11]

4. Summary

Although high-interstitial-alloyed austenitic steels with combined addition of N + C provide a variety of excellent properties of high strength, good ductility and toughness as well as improved corrosion resistance, they show a ductile-to-brittle transition as in the case of high-nitrogen austenitic steels. With the same interstitial content, however, the N + C alloyed steel had a lower DBTT than the N alloyed steel because the combined addition of N +

C enhances the metallic character of interatomic bonds and also lower N content contributes to the decrease of DBTT. When the austenite stability of high-interstitial-alloyed austenitic steels is decreased due to the low content of substitutional elements, on the other hand, DIMT can easily occur and thus increase DBTT by decreasing low-temperature toughness. To improve their strength and low-temperature toughness simultaneously, therefore, systematic studies are required for finding optimum contents of interstitial and substitutional elements in high-interstitial-alloyed austenitic steels.

Acknowledgements

The study was financially supported by the Ministry of Knowledge Economy. The authors would like to thank Mr. Jong-In Bae of Korea Institute of Materials Science for his help with vacuum-induction melting and heat treatments.

References

- [1] Speidel MO. From high-nitrogen steels (HNS) to high-interstitial alloys (HIA). In: Speidel MO, Kowanda C, Diener M, editors. *HNS 2003 - High nitrogen steels*, Schaffhausen, Switzerland: Institute of Metallurgy ETH Zürich; 2003, p. 1-8.
- [2] Gavriljuk VG, Berns H. High nitrogen steels. Berlin: Springer-Verlag; 1999.
- [3] Akdut N, De Cooman BC, Kim HS. Proceedings of 1st International Conference on interstitially alloyed steels, IAS 2008, Pohang, Korea, 2008.
- [4] Gavriljuk VG, Shanina BD, Berns H. A physical concept for alloying steels with carbon + nitrogen. *Mater Sci Eng* 2008;**481-482**:707-712.
- [5] Müllner P, Solenthaler C, Uggowitzer PJ, Speidel MO. Brittle fracture in austenitic steel. *Acta Mater* 1994;**42**:2211-7.
- [6] Tomota Y, Xia Y, Inoue K. Mechanism of low temperature brittle fracture in high nitrogen bearing austenitic steels. *Acta Mater* 1998;**46**:1577-87.
- [7] Uggowitzer PJ, Magdowski R, Speidel MO. Nickel free high nitrogen austenitic steel. *ISIJ Int* 1996;**36**:901-8.
- [8] Balachandran G, Bhatia ML, Ballal NB, Krishna RAO P. Some theoretical aspects on designing nickel free high nitrogen austenitic stainless steels. *ISIJ Int* 2001;**41**:1018-27.
- [9] Speidel MO, Zheng-Cui M. High-nitrogen austenitic stainless steels. In: Speidel MO, Kowanda C, Diener M, editors. *HNS 2003 - High nitrogen steels*, Schaffhausen, Switzerland: Institute of Metallurgy ETH Zürich; 2003, p. 63-73.
- [10] Bernauer J, Saller G, Speidel MO. Combined influence of carbon and nitrogen on the mechanical and corrosion properties of Cr-Mn steel grades. In: Akdut N, De Cooman BC, Fock J, editors. *Proceedings of the 7th International Conference on High nitrogen steels – HNS 2004*, Ostend, Belgium: GRIPS media GmbH; 2004, p. 529-37.
- [11] Frehn A, Ratte E, Wolfgang B. Influence of temperature and strain rate on the mechanical and the formability of the austenitic stainless steel 1.4376 containing manganese and nitrogen. In: Akdut N, De Cooman BC, Fock J, editors. *Proceedings of the 7th International Conference on High nitrogen steels – HNS 2004*, Ostend, Belgium: GRIPS media GmbH; 2004, p. 447-60.
- [12] Karjalainen LP, Taulavuori T, Sellman M, Kyröläinen. Some strengthening methods for austenitic stainless steels. *Steel Research Int* 2008;**79**:404-12.
- [13] Hwang B, Lee T-H, Kim S-J. Effect of deformation-induced martensite and grain size on ductile-to-brittle transition behavior of austenitic 18Cr-10Mn-N stainless steels. *Met Mater Int* 2010;**16**:905-11.
- [14] Tobler RL, Meyn D. Cleavage-like fracture along slip planes in Fe-18Cr-3Ni-13Mn-0.37N austenitic stainless steel at liquid helium temperature. *Metall Mater Trans* 1988;**19A**:1626-31.
- [15] Lee T-H, Shin E, Oh C-S, Ha H-Y, Kim S-J. Correlation between stacking fault energy and deformation microstructure in high-interstitial-alloyed austenitic steels. *Acta Mater* 2010;**58**:3173-86.
- [16] Talonen J, Hänninen H. Formation of shear bands and strain-induced martensite during plastic deformation of metastable austenitic stainless steels. *Acta Mater* 2007;**55**:6108-18.
- [17] Zhang MX, Kelly PM. Relationship between stress-induced martensitic transformation and impact toughness in low carbon austenitic steels. *J Mater Sci* 2002;**37**:3603-13.
- [18] Antolovich SD. Fracture toughness of strain-induced phase transformations. *Trans TMS-AIME* 1968;**242**:2371-3.